

IONOSPHERIC ERROR REMOVAL IN THE POSITIONING OF LEO SATELLITES BASED ON LOW COST GPS RECEIVERS

Oliver MONTENBRUCK
Eberhard GILL

*Deutsches Zentrum für Luft- und Raumfahrt (DLR), German Space Operations Center
82234 Wessling, Germany
oliver.montenbruck@dlr.de*

ABSTRACT – *A novel technique for the ionospheric correction of single frequency GPS measurements from satellites in low Earth orbit (LEO) is presented. The fractional total electron content (TEC) above the receiver altitude is obtained from global TEC maps of the IGS network and an altitude dependent scale factor. By choosing a suitable effective height of the residual ionosphere, the resulting path delay for positive elevations from the LEO satellite to the GPS satellites is computed using a thin layer approximation. The scale factor can either be predicted assuming a Chapman profile for the altitude variation of the electron density or adjusted as a free parameter in the processing of an extended set of single frequency measurements. Based on flight data from the Champ satellite, that orbits the Earth at an altitude of 450 km, the developed algorithm allows for a 90% correction of the ionospheric error in a reduced dynamic orbit determination, based on single frequency C/A code measurements.*

KEYWORDS: Ionosphere, GPS, LEO satellites, orbit determination, Champ

INTRODUCTION

The increasing availability of flight-proven and affordable GPS receivers for space applications has rendered GPS a widely accepted tracking system for LEO satellites [1-4]. Following the switch-off of the Selective Availability of the GPS satellites in May 2000 [5], common L1 C/A code receivers can now provide position information in the 1-10 m accuracy region, which is mainly limited by the ionospheric refraction. Thus, the removal of ionospheric effects is a major prerequisite for an improved orbit reconstruction of LEO satellites equipped with low cost single frequency GPS receivers.

To this end, an ionospheric correction model is introduced, which makes use of global total electron content (TEC) maps from the IGS network. Modeling the altitude dependency of the electron density by a Chapman profile allows in turn to estimate the fractional TEC above the receiver altitude. The ionospheric path delay for positive elevations is then obtained from a thin layer approximation with a suitably chosen effective height of the residual ionosphere above the receiver.

Flight data from the Champ satellite which orbits the Earth at an altitude of 450 km are applied to validate the proposed model. Since Champ carries a dual frequency GPS receiver, a direct measurement of the ionospheric range delay is available from P1 and P2 pseudoranges, that serves as a reference for the proposed model.

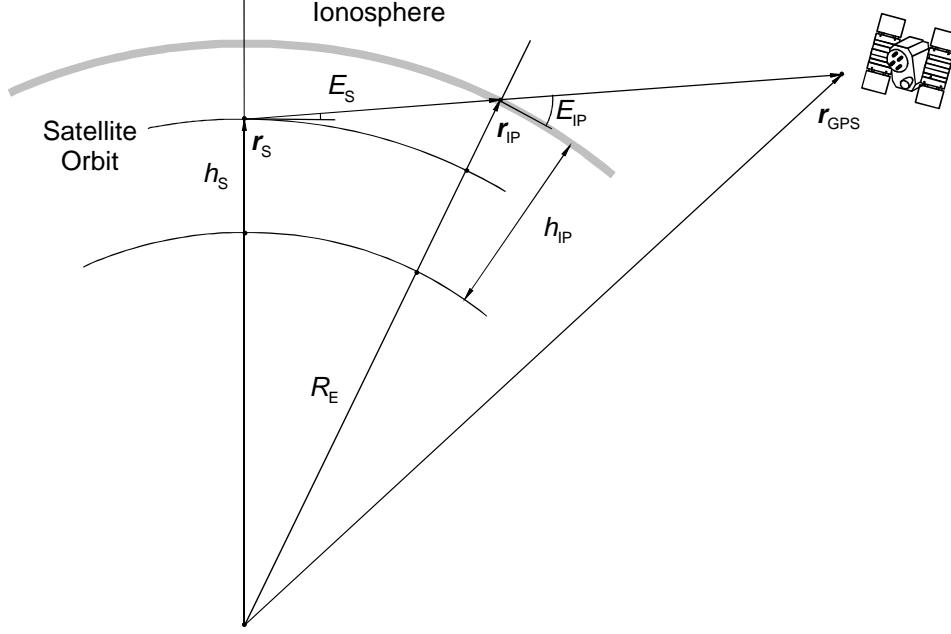


Fig. 1 Geometry of thin layer ionosphere correction model for satellite orbits

IONOSPHERIC CORRECTION MODEL

A single layer approximation, commonly adopted for the ionospheric correction of terrestrial GPS measurements, is applied to describe the ionospheric path delay of spaceborne pseudorange measurements. To this end the residual ionosphere above the satellite is assumed to be concentrated in a single layer at altitude $h_{IP} > h_S$, with h_S being the satellite altitude above the Earth's surface. As depicted in Fig. 1, the signal received by the user spacecraft at location \mathbf{r}_S with a positive elevation E_S traverses the spherical ionospheric layer once at the ionospheric point (IP) with elevation $E_{IP} \geq E_S$. Hence pseudorange measurements taken at the L1 frequency (f_{L1}) experience a group delay

$$\Delta \mathbf{r}_{L1} = \frac{1}{\sin(E_{IP})} \frac{40.3 \text{ m}^3 \text{ s}^{-2}}{f_{L1}^2} \text{TEC}(\mathbf{r}_{IP}) = \frac{0.162 \text{ m}}{\sin(E_{IP})} \frac{\text{TEC}(\mathbf{r}_{IP})}{10^{-16} \text{ m}^{-2}} = \mathbf{a} \frac{0.162 \text{ m}}{\sin(E_{IP})} \frac{\text{TEC}(\mathbf{l}_{IP}, \mathbf{j}_{IP}, 0)}{10^{-16} \text{ m}^{-2}} \quad (1)$$

where $\text{TEC}(\mathbf{r}_{IP})$ denotes the total electron content at IP and \mathbf{a} is a scaling factor for the ratio of the $\text{TEC}(\mathbf{l}_{IP}, \mathbf{j}_{IP}, h_{IP})$ above altitude h_{IP} and the $\text{TEC}(\mathbf{l}_{IP}, \mathbf{j}_{IP}, 0)$ above ground. Here, the mapping function

$$M(E_{IP}) = \frac{1}{\sin(E_{IP})} = \left\{ 1 - [\cos(E_S) r_S / r_{IP}]^2 \right\}^{-1/2} \quad (2)$$

accounts for the increase of the path length in the ionosphere with decreasing elevation (cf. [6]). It is noted, that the geographical coordinates of the ionospheric point and the elevation of the line-of-sight vector depend on the positions of the user satellite and the GPS satellite as well as the adopted reference height h_{IP} of the residual ionosphere.

While the geographical variation $\text{TEC}(\mathbf{I}_{\text{IP}}, \mathbf{j}_{\text{IP}}, 0)$ of the total electron content is readily accessible today from ground-based observations of GPS satellites, the restitution of the vertical stratification of the ionosphere is severely limited by the restricted observation geometry (cf. [7]). Reference to theoretical models like the International Reference Ionosphere IRI95 (cf. [8]) must therefore be made to obtain information on the altitude variation of the ionospheric electron density. Its use is complicated, however, since the predicted density values do not converge to zero within the limited altitude range of the model (1000 km). To circumvent the considerable uncertainty in the prediction of the effective altitude and the total electron content of the residual ionosphere in the IRI95 model, a Chapman profile is applied to fit the IRI95 values. Defining the effective altitude of the residual ionosphere as the 50 percentile altitude, the scaling factor is

$$\mathbf{a} = \frac{1}{2} \frac{e - \exp(1 - \exp(-(h_s - h_0)/H))}{e - \exp(1 - \exp(-h_0/H))} \quad (3)$$

where h_0 and H are the suitably adjusted inflection point altitude and the scale height of the Chapman profile, respectively.

A sample Chapman profile with inflection point height $h_0 = 420$ km and scale height $H = 100$ km is illustrated in Fig. 2. It provides a close approximation of the IRI95 density values on Aug. 7, 2000 near the location of the global TEC maximum.

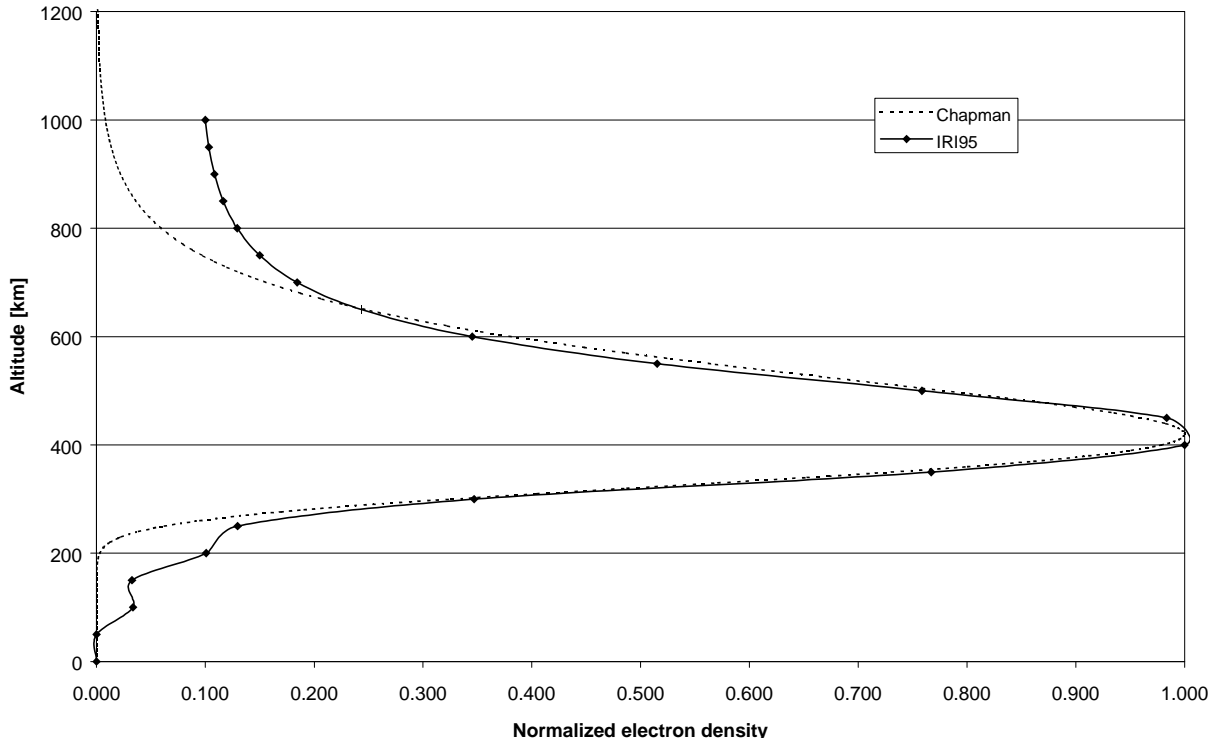


Fig. 2 IRI95 normalized electron density profile near the global TEC maximum on Aug. 7, 2000 ($j=0^\circ$, $\lambda=-140^\circ$, $t=01:00$ UTC). The density variation is best represented by a Chapman profile with scale height $H = 100$ km and inflection point height $h_0 = 420$ km.

CHAMP DATA SET

The Champ micro satellite, launched on July 15, 2000, orbits the Earth at an altitude of 450 km and is the first of a series of scientific and remote sensing satellites equipped with a geodetic quality GPS receiver developed by the Jet Propulsion Laboratory. Key mission goals comprise the derivation of accurate and

self-contained gravity field models as well as limb sounding of the Earth atmosphere [9]. The Blackjack receiver onboard Champ is a cross-correlation GPS receiver providing code and phase measurements on both the L1 and L2 frequency [10]. It is a follow-on of the Turbo-Rogue receiver previously flown on e. g. the Microlab-1 mission as part of the GPS/MET project (see e.g. [2]).

A first set of GPS measurements and an associated reference trajectory was released in early December 2000 by the Champ project [11]. The data, which have been collected on August 7, 2000, cover 24 hours of measurements at a rate of one value per 10 s. For the ionosphere free linear combinations of L1 and L2 P code pseudoranges, an error of 1.3 m (rms) has been determined [10].

In the framework of the study, the L1/L2 P code pseudoranges are applied for calibration and verification of the proposed correction model, while the C/A code measurements, in contrast, serve as an independent data set, which is considered to be representative of common single frequency receivers. Furthermore, a rapid science orbit provides a precise reference trajectory for the concerned time interval.

ANALYSIS AND RESULTS

Comparison with Observed Ionospheric Path Delays

The modeled group delay of C/A code pseudoranges based on (1) may be compared with the observed ionospheric path delays using L1 and L2 P code pseudoranges. Since the ionosphere is a dispersive medium, the difference in delay between the L2 and the L1 pseudoranges can be used to determine the absolute delay at the primary L1 frequency to high accuracy. Making use of Chapman profiles adjusted to the IRI95 density values for Aug 7, 2000, an effective altitude of 540 km (570 km) and a 50% (40%) percent fraction of the total electron content measured at ground are expected for the residual ionosphere above a satellite at altitude 450 km near the global TEC maximum (minimum). Accurate TEC values for the day of interest have furthermore been made available by the Center of Orbit Determination in Europe (CODE) in Berne (see [12]).

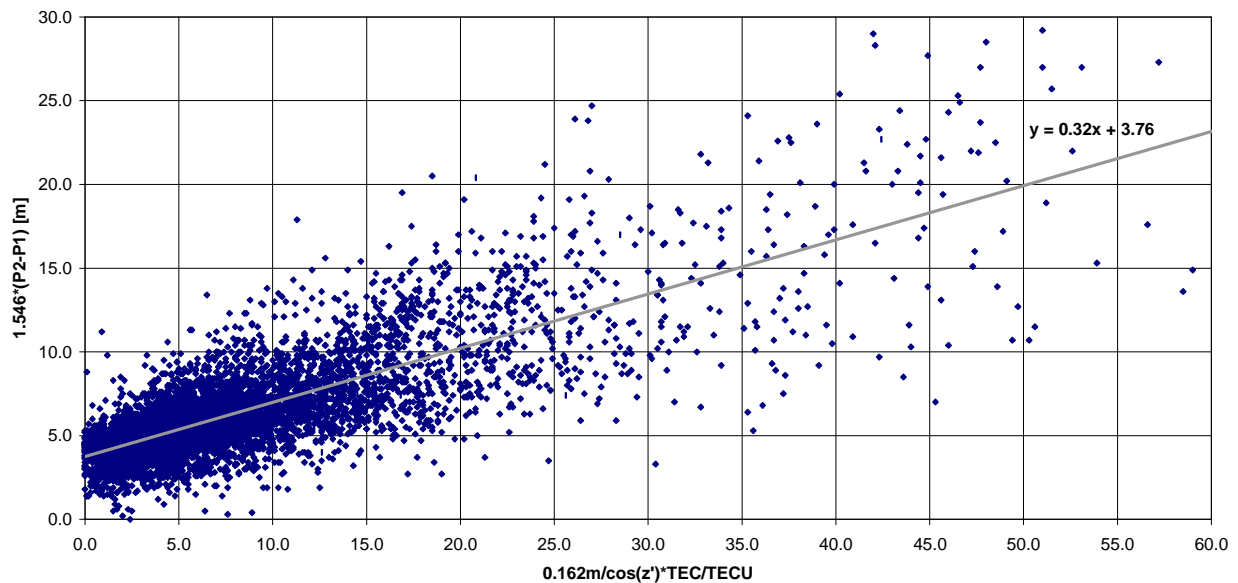


Fig. 3 Calibration of the differential code bias and the fractional TEC of the ionosphere above the Champ altitude using ionospheric range delay residuals

To assess the quality of the proposed model, the measured ionospheric path delays (restricted to elevations above 10°) have been compared against predicted values assuming a reference height $h_0 = 550$ km and a fractional TEC of $a = 1$. The results shown in Fig. 3 show a good overall correlation, which is best represented by a linear relation with an offset of 3.8 m and a slope of 0.32.

The calibrated offset of 3.8 m indicates a differential code bias (DCB) of 2.4 m or, equivalently, 8 ns between the L2 and L1 code phase measurements of the Champ Blackjack receiver. The empirical calibration $a^{\text{calib}} = 0.32$ of the fractional electron content of the ionosphere above the Champ orbit differs notably from the substantially smaller predicted value $a^{\text{pred}} = 0.40..0.50$ expected from the IRI95 model, which indicates a practical limitation of a purely model based ionospheric correction. Thus, an adjustment of the scaling factor a in a single point positioning or a dynamic orbit determination is clearly preferable.

C/A Code Single Point Positioning

Based on IGS precise GPS orbits and clock solutions, Champ kinematic point positions and Blackjack receiver clock offsets have been obtained. Making use of 24 hours of pseudorange data collected on Aug. 7, 2000, sampled at 60 s, the position coordinates and the receiver clock offset were estimated in an unconstrained least-squares adjustment at each measurement time step. Modeled pseudoranges have been corrected for the GPS satellite clock offset, the relativistic GPS satellite clock offset and the GPS satellite antenna offset.

Care has been taken to remove the frequent outliers of the receiver (10 m to 100 km), to discard all measurements collected below an elevation limit of 10° , to ignore data points with residuals exceeding a threshold of 2.5 m, and to reject measurements with position-dilution-of-precision (PDOP) values larger than 10.

The resulting mean and r.m.s. position errors and their components in radial, east and north direction are summarized in Table 1. Case 1, based on L1 band C/A code measurements with measured ionospheric corrections from L2/L1 P code differences, illustrates the achievable position accuracy of about 2 m in the horizontal plane and 3 m in the radial direction.

Table 1 Point positioning accuracy for the Champ satellite. Data type keys C1, P1 and P2 designate C/A code pseudoranges, L1 P code pseudoranges and L2 P code pseudoranges, respectively.

Case	Data type	Ionospheric Correction	Position [m]		Radial [m]		East [m]		North [m]	
			mean	r.m.s.	mean	r.m.s.	mean	r.m.s.	mean	r.m.s.
1	C1	P2-P1 difference	2.89	2.61	+0.21	3.44	-0.06	0.84	+0.03	1.61
2	C1	TEC map (CODE), $\alpha=0.32, h_0=550\text{km}$	3.20	2.28	+0.27	3.49	-0.20	0.92	-0.05	1.50
3	C1	None	4.58	3.13	+3.58	3.84	-0.12	0.96	-0.04	1.51

The achievable accuracy of the proposed ionospheric correction model is illustrated in case 2. Here, ionospheric path delays have been predicted from two dimensional TEC maps obtained from CODE and used to correct the C/A code pseudoranges. The computation was performed with an assumed value of $h_0 = 550$ km for the effective height of the residual ionosphere and the best-fit value $a^{\text{calib}} = 0.32$ was adopted for the fractional TEC above the Champ orbit. The accuracies of the obtained point solution differ only slightly from case 1 and provide a justification of the model and its inherent assumptions and simplifications. A small offset of 0.20 m in the East/West component is apparently caused by an asymmetric orientation of the Champ orbit with respect to the ionospheric bulge and a non-uniform quality of the model for different locations.

On the other hand, application of the predicted corrections to the single frequency C/A code measurements evidently offers a notable accuracy gain over the use of uncorrected pseudoranges. As illustrated by a comparison of cases 2 and 3, the ionospheric correction essentially removes a systematic radial bias of 3.7 m, which is otherwise present in the C/A code position solution.

C/A Code Sequential Filtering

The analysis performed above demonstrates the overall validity of the proposed ionospheric correction model for LEO satellites. However, it is unrealistic in the sense that the optimum value of \mathbf{a} has been adjusted from dual frequency measurements, which in practice are not available when using a simple L1 C/A code receiver. Since a prediction of \mathbf{a} based on the IRI95 model yields unsatisfactory results, the calibration of \mathbf{a} from single frequency C/A code measurements is therefore studied in the sequel.

Based on the functional dependence of the ionospheric range correction on the relative location of the user satellite and the GPS satellite described in (1), the fractional electron content \mathbf{a} represents a single common scaling parameter for all observations, that can be adjusted to minimize the overall pseudorange residuals. A sequential batch filter has been chosen for the practical implementation of single point positioning with fractional TEC calibration. Starting from an assumed initial values of $\mathbf{a} = 0.5$ and $\mathbf{s}(\mathbf{a}) = 0.1$, the filter converges to a final value of $\mathbf{a}^{\text{est}} = 0.26$ (cf. Fig. 4), which is notably less than the result obtained from P2-P1 observations in the previous section. As a consequence, the resulting position estimates exhibit a systematic radial offset of about 1 m and hence accounts for merely 73% of the total effect on the computed single point position solutions.

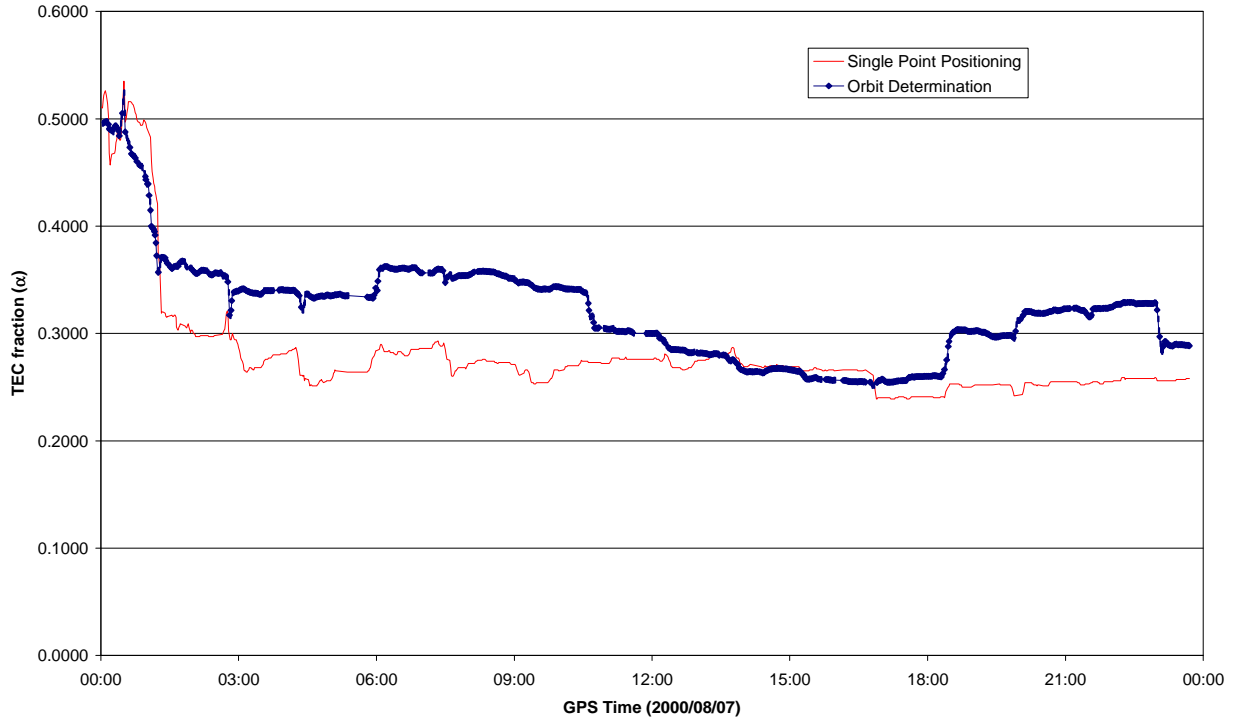


Fig. 4 Sequential filtering of the ionospheric scale factor \mathbf{a} from Champ C/A code pseudoranges

Better results are obtained when the Champ C/A code pseudoranges are processed in a reduced dynamic orbit determination. Here, the deterministic part of the applied force model comprises the Earth's gravity field up to degree and order 50, the luni-solar gravitation, the solar radiation pressure and atmospheric drag. Since neither the selected JGM-3 gravity field model [13] nor the simplifying Harries-Priester drag model [14] provide a sufficiently accurate representation of the actual perturbations affecting a satellite in a 450 km altitude orbit, empirical accelerations in the radial, along-track and cross-track directions have, furthermore, been considered in the analysis. The Kalman filter parameters comprise the 6-dimensional state vector (\mathbf{r}, \mathbf{v}) of the satellite, the GPS receiver clock error $(c\Delta t)$, the 3-dimensional vector of empirical accelerations $(\mathbf{a}_{\text{emp}})$, and, optionally, the ionospheric scaling parameter (\mathbf{a}) . In view of evident correlations

with the adjusted accelerations, the drag and solar radiation pressure coefficient have been held fixed at suitable a priori values.

As shown in Table 2, the errors of the filtered trajectory exhibit a notably smaller scatter than the single point solutions. This is particularly true for the radial component, which otherwise exhibits an unfavorable geometric dilution of precision and benefits most from the constraints introduced by the dynamical model. Using observed ionospheric corrections from dual frequency measurements, resulting r.m.s. errors of about 0.7 m are achieved in each axis (case 1).

Table 2 Accuracy of reduced dynamic orbit determination for Champ

Case	Data type	Ionospheric Correction	Position [m]		Radial [m]		East [m]		North [m]	
			mean	r.m.s.	mean	r.m.s.	mean	r.m.s.	mean	r.m.s.
1	C1	P2-P1 difference	1.05	0.55	+0.18	0.69	-0.02	0.67	-0.00	0.67
2	C1	α estimated, $\alpha_0=0.30$	1.77	0.92	+0.35	1.31	-0.28	0.86	+0.04	1.15
3	C1	None	4.00	1.36	+3.58	1.46	-0.33	1.12	+0.01	1.24

Upon adjusting the ionospheric scale parameter \mathbf{a} along with the other filter parameters, it takes about 1 revolution (1.5 hours) to achieve convergence from initial conditions of $\mathbf{a}_0 = 0.5$ with standard deviation $\mathbf{s}(\mathbf{a}_0) = 0.1$ (cf. Fig. 4). Major jumps in the estimated value may be observed once per orbit coinciding with TEC maxima at the crossing of the ionospheric bulge. Compared to the single point positioning, the estimated scaling parameter is generally higher, which reflects in a better performance of the ionospheric correction model. As shown in case 2, the adjustment of the TEC scaling parameter as part of the dynamical filtering (using a starting value of $\mathbf{a}_0 = 0.3$) yields a trajectory with a mean radial offset of 0.34 m. Considering that the use of uncorrected C/A code measurements results in a 3.6 m offset (case 3), the model thus accounts for roughly 90% of the total ionospheric effects.

SUMMARY AND CONCLUSIONS

In combination with global, 2-dimensional TEC maps, the thin-layer approximation of the ionosphere above a LEO satellite provides a suitable model for the ionospheric correction of single frequency pseudorange measurements from spaceborne GPS receivers. Aside from the effective height of the residual ionosphere, which may be derived from existing ionospheric models with adequate accuracy, the model involves an altitude dependent scaling factor for the fraction of the ground based total electron content.

For practical applications, the accuracy of the model is limited by the capability to adjust the TEC scaling factor from an extended set of single frequency observations or to predict its value from independent ionospheric models. Restricting oneself to C/A code pseudoranges, optimum results have been obtained in a dynamic orbit determination, in which the fractional TEC above the satellite orbit is estimated along with other state parameters. Here a 90% correction of the total ionospheric effects on the filtered trajectory has been demonstrated for the sample Champ data set.

ACKNOWLEDGMENT

The present study makes extensive use of Blackjack GPS receiver measurements that have been made available by GFZ, Potsdam, and JPL, Pasadena. Ionospheric TEC data employed in the analysis have, furthermore, been provided by CODE, Berne, as part of the IGS. The authors are grateful to M. Rothacher for technical discussions and valuable comments on the subject of GPS based positioning and orbit determination.

REFERENCES

- [1] Hart R.C., Gramling C.J., Deutschmann J.K., Long A. C., Oza D.H., Steger W. L.; *Autonomous Navigation Initiatives at the NASA GSFC Flight Dynamics Division*; 96-c-23; Proceedings of the 11th IAS (International Astrodynamics Symposium), May 1996 Gifu, Japan, 125-130 (1996).
- [2] Bisnath S.B., Langley R.B.; *Assessment of the GPS/MET TurboStar GPS receiver for orbit determination of a future CSA micro/small-satellite mission*; Dept. of Geodesy and Geomatics Engineering, Univ. New Brunswick, Contract No. 9F011-5-0651/001/XSD (1996).
- [3] Gill E., Montenbruck O., Brieß K.; *GPS-Based Autonomous Navigation for the BIRD Satellite*; 15th International Symposium on Spaceflight Dynamics, 26–30 June 2000, Biarritz (2000).
- [4] Unwin M.J., Oldfield M.K., Purivigraipong S.; *Orbital Demonstration of a New Space GPS Receiver for Orbit and Attitude Determination*; Int. Workshop on Aerospace Apps. of GPS; 31 Jan. – 2 Feb. 2000 Breckenridge, Colorado (2000).
- [5] White House; *Statement By the President Regarding the United States Decision to Stop Degrading Global Positioning System Accuracy*; Office of the Press Secretary; <http://www.whitehouse.gov/library/PressPreleases.cgi>; May 1st (2000).
- [6] Hofmann-Wellenhof B., Lichtenegger H., Collins J.; *Global Positioning System Theory and Applications*; Springer-Verlag Wien New York, 4th ed. (1997).
- [7] Kleusberg A.; *Atmospheric Models from GPS*; in Teunissen P.J.G., Kleusberg A., GPS for Geodesy; Springer Verlag, Heidelberg; 2nd ed. (1998).
- [8] Bilitza D., Koblinsky C., Beckley B., Zia S., Williamson R.; *Using IRI for the Computation of Ionospheric Corrections for Altimeter Data Analysis*; Adv. Space. Res. Vol. 15/2, 113–119 (1995).
- [9] Reigber Ch., Bock R., Förste Ch., Grunwaldt L., Jakowski N., Lühr H., Schwintzer P., Tilgner C., *CHAMP Phase B - Executive Summary*; Scientific Technical Report STR96/13 , GeoForschungsZentrum Potsdam (1996).
- [10] Kuang D., Bar-Sever Y., Bertiger W., Desai S., Haines B., Meehan T., Romans L.; *Precise Orbit Determination for CHAMP using GPS Data from BlackJack Receiver*; ION National Technical Meeting, Paper E1-5, January 22-24, Long Beach, California (2001).
- [11] Champ Newsletter No. 2; <http://op.gfz-potsdam.de/champ>; Dec 8, (2000).
- [12] AIUB; *Global Ionosphere Maps (GIMs) Produced by CODE*; <http://www.aiub.unibe.ch/ionosphere.html>.
- [13] Tapley B.D., Watkins M.M., Ries J.C., Davis G.W., Eanes R.J., Poole S.R., Rim H.J., Schutz B.E., Shum C.K., Nerem R.S., Lerch F.J., Marshall J.A., Klosko S.M., Pavlis N.K., Williamson R.G.; *The Joint Gravity Model 3*; Journal of Geophysical Research 101, 28029–28049 (1996).
- [14] Long A.C., Cappellari J.O., Velez C.E., Fuchs A.J.; *Mathematical Theory of the Goddard Trajectory Determination System*; Goddard Space Flight Center; FDD/552-89/001; Greenbelt, Maryland (1989).